

Supplementary Information for Formation and prevention of fractures in sol-gel-derived thin films

Emiel J. Kappert,^a Denys Pavlenko,^a Jürgen Malzbender,^b Arian Nijmeijer,^a Nieck E. Benes,^{*a} and Peichun Amy Tsai^{*c}

Received 16th September 2014, Accepted Xth XXXXXXXXXX 20XX

First published on the web Xth XXXXXXXXXX 200X

DOI: 10.1039/b000000x

1 Details on determining crack density

The following sequence of steps was taken for the image analysis of the crack edge, with Matlab built-in functions:

1. Edge detection with the Laplacian of Gaussian filter on the grayscale image. The edge detection results in a binary matrix, where the 1s represent the outlines of the cracks and the 0s represent the space in between.
2. Removal of regions (regions of 1s that are connected) with less than 30 pixels from the matrix obtained in step 1, as these regions with only a few pixels were heuristically determined to constitute noise;
3. Removal of regions for which the extent (the ratio of 1s to the number of total pixels in the bounding box) is higher than 0.05, as these regions with a bounding box that is comparatively small to the amount of pixels were heuristically determined to constitute noise;
4. To convert the outlines of the cracks to a single-pixel crack line, the following morphological operations were used: a. Filling of the isolated interior pixels; b. Dilation with a 3x3 matrix of ones; c. Bridging, setting 0s with at least two non-zero non-connected neighbours to 1; d. Dilation with a 3x3 matrix of ones; e. Setting 0s to 1 if 5 or more of its 3x3 neighbours are 1; f. Thinning with $n = \text{Inf}$, shrinking objects down to lines; g. Filling of the isolated interior pixels;

This sequence was heuristically determined to result in an accurate representation of the cracks by a single line.

^a Inorganic Membranes Group, University of Twente, MESA⁺ Institute for Nanotechnology and Faculty of Science and Technology, PO Box 217, 7500 AE Enschede, The Netherlands; E-mail: n.e.benes@utwente.nl

^b Forschungszentrum Jülich GmbH, IEK-2, 52425 Jülich, Germany.

^c Soft matter, Fluidics and Interfaces Group, University of Twente, MESA⁺ Institute for Nanotechnology, PO Box 217, 7500 AE Enschede, The Netherlands; E-mail: p.a.tsai@utwente.nl

2 Details on determining crack spacing

The image obtained in step 4g above was used as a starting point for the determination of the crack spacing. Crack spacing was determined via two individual approaches. Both approaches involve the determination of the Euclidian distance transform of the binary image. The distance to the nearest white pixel is determined by: $\sqrt{(x_1 - x_2)^2 + (y_1 - y_2)^2}$. A plot of this distance transform is given in Figure 3C in the main paper, where blue colors indicate regions close to cracks and red colors regions far away from cracks.

Method 1

In the first method to determine the crack spacing, the average value of the Euclidian distance transform was taken as a measure for the crack spacing. This method will always underestimate the crack spacing because it averages over the pixels close to the cracks as well.

Method 2

In the second method, the midpoint between two lines was determined by performing a watershed analysis, where the different cracks were used as catchment basins. The result of this analysis are watershed lines, i.e., lines that are at exactly in between two cracks. In this method, the crack distance was taken as the average distance to the cracks on the watershed lines.

Method 2 represents a more accurate calculation of the crack distance, but may omit the crack spacing of regions that are enclosed by a single crack. Therefore, the results of method 2 were checked against the results of method 1, and confirmed to give the similar results. Therefore, the results of method 2 were taken as a representative value for the average crack spacing in an image.

Table 1 Mechanical properties for silica and BTESE after drying and after annealing, measured by nanoindentation on layers supported on a silicon wafer. The error bars denote the 95% confidence intervals over a large amount of indentations in a single sample. Because of the low layer thicknesses, cautiousness is required upon interpreting the data (see text). Explanation of symbols: E^* , plane-strain modulus; H_{max} , maximum creep during holding for 20 seconds at maximum force; μIT , elastic contribution to the total work;

	Layer thickness (nm)	Indentation hardness (N/mm)	Vickers hardness (HV)	E^* (GPa)	H (nm)	CIT (%)	μIT (%)
Silica	194	415±29	39±3	6.1 ± 0.7	134 ± 5	12±2	35±4
Silica	153	606±76	56±7	10.9 ± 1.2	111 ± 8	9±1	28±4
Silica (calcined)	191	447±26	41±2	6.5 ± 0.4	128 ± 5	12±1	39±3
Silica (calcined)	76	532±37	49±3	7.1 ± 0.4	112 ± 7	14±2	39±2
BTESE	1182	476±49	39±4	7.6 ± 1.1	136 ± 8	9±1	27±5
BTESE (calcined)	946	426±43	43±3	5.8 ± 0.5	135 ± 7	12±1	39±5

3 Nanoindentation measurements

Table S1 lists the mechanical properties for silica and BTESE as determined by nanoindentation measurements performed in this study. The layers used for the nanoindentation measurements needed to stay (well) below the critical thickness, requiring low layer thicknesses. However, a lower layer thickness results in increased effect of the substrate properties on the measurement results. Typically, for measuring the elastic properties, the indentation depth H_{max} should be smaller than 10% of the layer thickness. For measuring the layer hardness, a deeper indentation is allowed. Especially in the case of the silica layers, the indentation depths over the layer are significantly above half of the layer thicknesses (69%, 73%, 67%, and 147%). The values obtained for silica should therefore be used as an estimate of the order of magnitude only.

ness h . For multiple orders of magnitude of film thicknesses, the ratio λ/h was found to be approximately 30. From our data, we calculate the ratio $W_1 = \lambda/h$ and find the average of λ/h of 34, which is consistent with a recent theoretical prediction¹. The agreement suggests that such periodic, wavy cracks stems from the interplay between layer delimitation and crack-ing propagation, quantitatively predicted by the collaborative model¹.

References

- 1 J. Marthelot, B. Roman, J. Bico, J. Teisseire, D. Dalmas and F. Melo, *Phys. Rev. Lett.*, 2014, **113**, 085502.

4 Correlation between replicating crack distance and film thickness

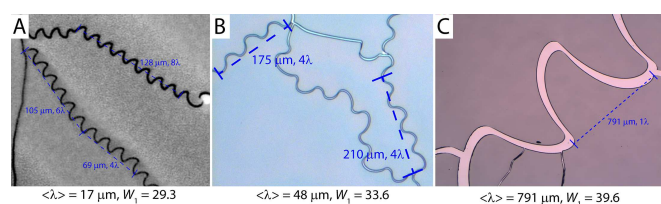


Fig. 1 Determination of the characteristic length scale for periodic cracks for three films of different thicknesses: A: a 575 ± 10 nm silica film; B: a 1430 ± 140 nm BTESE-derived organosilica film; and C: a 20 ± 2 μm BTESE-derived organosilica film.

In Figure 1, we show the characteristic length scale, λ , for periodic cracks in three films of different thicknesses. One of the films is silica, the other two films are made of BTESE-derived organosilica. A recent study¹ identified a relationship between the crack replicating distance W_1 and the film thick-